Augmentation of Wind Farms Ride Through by DFIG-based Variable Speed Wind Generators

K. E. Okedu*, S. M. Muyeen, R. Takahashi* and J. Tamura***

Abstract – Wind farm grid codes require wind generators to ride through voltage sags, which means that normal power production should be re-initiated once the nominal grid voltage has been recovered. Doubly Fed Induction Generator (DFIG) based wind farm is gaining popularity these days because of its inherent advantages like variable speed operation and independent controllability of active and reactive power over conventional Induction Generator (IG). This paper proposes a new control strategy using DFIGs for stabilizing a wind farm composed of DFIGs and IGs. Simulation analysis by using PSCAD/EMTDC shows that the DFIGs can effectively stabilize the IGs and hence the entire wind farm through the proposed control scheme by providing sufficient reactive power to the system.

Keywords: DFIG, IG, Grid fault, Wind energy, Wind farms

1. Introduction

Emerging environmental concerns and attempts to curtail dependency on fossil fuel resources are bringing the renewable energy resources to the mainstream of the electric power sector. Among the various renewable resources, wind power is the most promising from technical and economical prospects. The response of wind generators to grid disturbances is an important issue, because the installations of wind generators are steadily increasing. Therefore, it is important for utilities to study the effects of various voltage sags on the corresponding wind turbine responses [1], [2]. The emerging grid codes demand that wind farms should have a good performance with respect to voltage control capability and robust behavior against frequency and voltage variations under fault condition. The installations of power electronic devices and reactive power compensation units like static synchronous compensator (STATCOM), superconducting magnetic energy storage (SMES), and energy capacitor system (ECS), in a wind farm composed of fixed speed wind turbines (FSWTs) as presented in [3]-[5], increase the system overall cost. The amount of necessary dynamic reactive power compensation depends generally on the type of wind turbine generator system (WTGS) considered and is influenced by the electrical and mechanical parameters of that unit. Therefore, it is paramount to use a variable speed wind turbine (VSWT) like a DFIG to stabilize a FSWT (IG) in a wind farm, because the DFIG system can also control reactive power in a similar manner to a STATCOM/SMES/ECS and thus the reactive power compensation can be implemented at a lower cost.

* Dept. of Elect/Elect Engineering, Kitami Instistute of Technology, Hokkaido, 090-8507, Japan. (kenokedu@yahoo.com, rtaka@mail.kitami-it.ac.jp, and tamuraj@mail.kitami-it.ac.jp)
** Dept. of Elect. Engineering, The Petroleum Institute, Abu Dhabi, UAE. (smmuyeen@pi.ac.ae)
Received 16 June 2011;Accepted 01 November 2011

2. Wind Turbine Model

A wind turbine is an electromechanical energy conversion device that captures kinetic energy from the wind and turns it into electrical energy. The primary components of a wind turbine for modeling purposes consist of the turbine rotor or prime mover, a shaft, and a gearbox unit (a speed changer) [6].

The dynamics interaction involving forces from the wind and the response of wind turbine determines the amount of kinetic energy that can be extracted. The aerodynamic torque and the mechanical power of a wind turbine are given by [7], [8], and [9].

$$T_M = \frac{\pi \rho R^3}{2} V_w{}^2 C_t(\lambda) \text{ [NM]} \tag{1}$$

$$P_M = \frac{\pi \rho R^2}{2} V_w{}^3 C_p(\lambda) \text{ [W]} \tag{2}$$

Where ρ is the air density, R is the radius of the turbine, V_w is the wind speed, $C_p(\lambda, \beta)$ is the power coefficient given by

$$C_p(\lambda, \beta) = 0.5(\Gamma - 0.02\beta^2 - 5.6)e^{-0.17\Gamma} \tag{3}$$

The relationship between C_t and C_p is

$$C_t(\lambda) = \frac{C_p(\lambda)}{\lambda} \quad (4)$$

$$\lambda = \frac{\omega_r R}{V_w} \quad (5)$$

In (3), $\Gamma = \frac{R}{\lambda}\frac{(3600)}{(1609)}$ and in (5), λ is the tip speed ratio.

The wind turbine characteristics [10] for both IGs and DFIGs are shown in Figs. 1 and 2 respectively. In Fig. 2, the power capture characteristic of the turbine and the rotor speed are shown. The dotted lines show the locus of the maximum power point of the turbine which is used to determine the reference of active power output P_{ref}. Equations (6) and (7) are used to calculate the reference of the active power output P_{ref} as shown in section A of Fig. 3. The optimum rotor speed ω_{ropt} is given in eqn. (8). The operation range of the rotor of DFIG is chosen from 0.7pu to 1.3pu as shown in the turbine characteristics in Fig. 2.

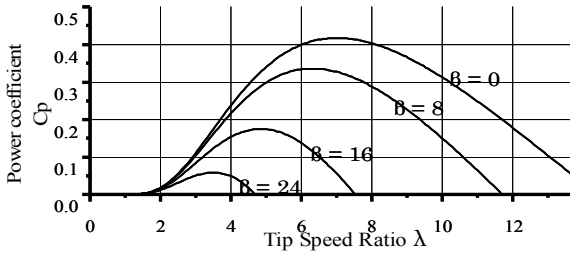

Fig. 1. C_P- λ curves for different pitch angles (for FSWT)

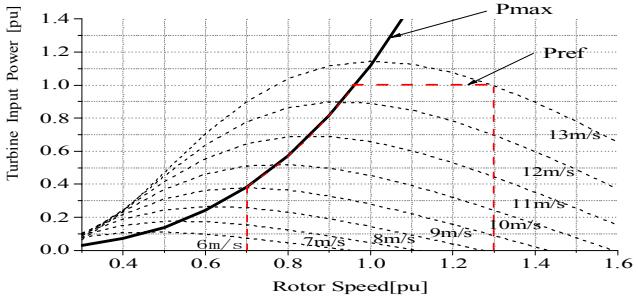

Fig. 2. Turbine characteristic with maximum power point tracking (for VSWT)

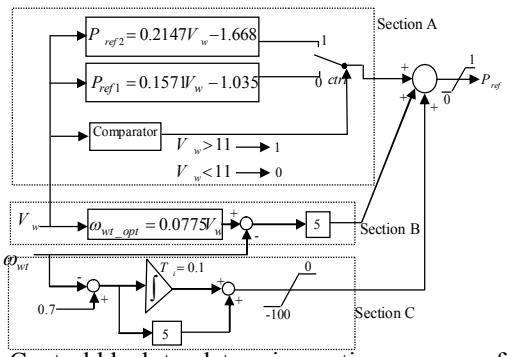

Fig. 3. Control block to determine active power reference P_{ref}

$$P_{ref1} = 0.1571V_w - 1.035 \quad [pu] \quad (7)$$

$$P_{ref2} = 0.2147V_w - 1.668 \quad [pu] \quad (8)$$

$$\omega_{ropt} = 0.0775V_w \quad [pu] \quad (9)$$

The power extracted from the wind can be limited by pitching the rotor blades. The angle control is usually done with a PI controller in such a way that the pitch controller shown in Fig. 4 controls the angle when the rotor speed exceeds 1.3pu for the case of DFIG that operates in variable speed mode. Figure 5 shows the pitch controller for the fixed speed WTGS. In order to get a realistic response in the pitch angle control system, the servomechanism account for a servo time constant, T_{servo} and a limitation of both the pitch angle and its rate of change as shown in Figs. 4 and 5 respectively. The rate of change limitation is very important during grid fault, because it decides how fast the aerodynamic power can be reduced in order to prevent over-speeding during fault [11], [12]. However, considering the realistic scenario for a heavy mechanical system, the rate limiter must be incorporated to simulate the pitch controller. The pitch rate limiter of ± 10deg. /sec. is used for both pitch controllers in this study.

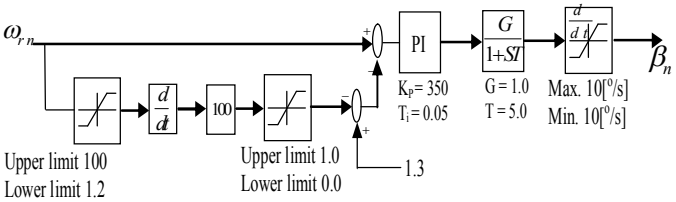

Fig. 4. Pitch controller for VSWT

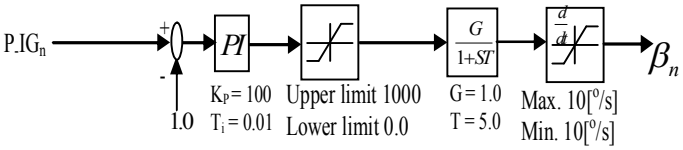

Fig. 5. Pitch controller for FSWT

3. Model System and Overview of DFIG Control

A model system shown in Fig. 6 is considered, in this study, where two wind farms are connected to the multi-machine power system. Aggregated wind farm model is considered in this analysis for fast computing. Each wind farm is composed of 1 DFIG and 3 IGs. The parameters of the generators are given in Table I. The basic control system of the DFIGs is presented in [7], but a protection circuit in the excitation circuit of DFIG is considered, in this study.

The two-mass shaft model is considered for all wind generator systems, because the shaft model has great influence on the fault analysis [13].

The IEEE generic turbine model and approximate mechanical-hydraulic speed governing system [14] is used for synchronous generator 1 (SG1). The IEEE "non-elastic water column without surge tank" turbine model and "PID control including pilot and servo dynamics" speed-governing system [15] is used for synchronous generator 2 (SG2). IEEE alternator supplied rectifier excitation system (ACIA) [16] is used in the exciter model of both synchronous generators.

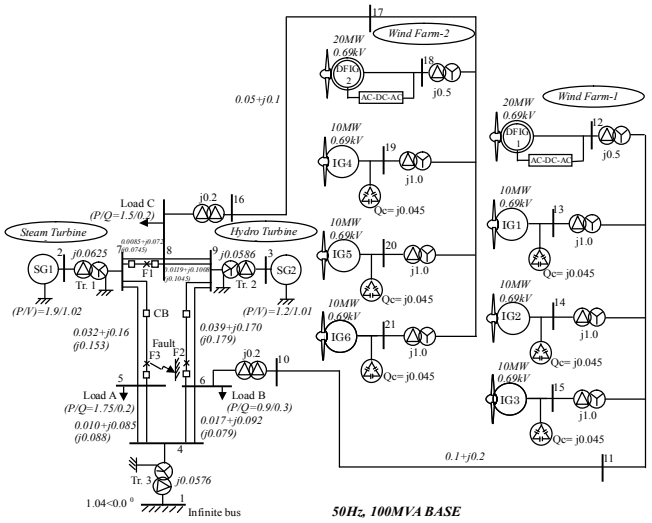

Fig. 6. Model system

Table 1. Generator Parameters

Generator Type	SG1	SG2	Generator Type	IGs	DFIGs
MVA	200	130	MVA	10	20
r_a (pu)	0.003	0.003	r1 (pu)	0.01	0.01
x_a (pu)	0.102	0.130	x1 (pu)	0.1	0.15
X_d (pu)	1.651	1.200	Xmu (pu)	3.5	3.5
X_q (pu)	1.590	0.700	r21 (pu)	0.035	0.01
$X^{/}_d$ (pu)	0.232	0.300	x21 (pu)	0.030	0.15
$X^{/}_q$ (pu)	0.380		r22 (pu)	0.014	
$X^{//}_d$ (pu)	0.171	0.220	x22 (pu)	0.098	
$X^{//}_q$ (pu)	0.171	0.250	Hg (pu)	0.3	0.3
$T^{/}$do (sec)	5.900	5.000	Hwt (pu)	3.0	3.0
$T^{/}$qo (sec)	0.535		Kw (pu)	90	90
$T^{//}$do(sec)	0.033	0.040			
$T^{//}$qo(sec)	0.078	0.050			
H (sec)	9.000	2.500			

DFIG has a superior characteristic than IG that both active and reactive powers can be controlled independently in the range of few milliseconds [17-20]. DFIG can also hold to some degree the electrical power constant in spite of fluctuating wind by storing temporarily the wind energy in the turbine as kinetic energy. The control systems are discussed below.

The circuit configuration of the rotor side, DC-link and the grid-side converter is given in Fig. 7, while Table 2 gives the ratings of the excitation circuit.

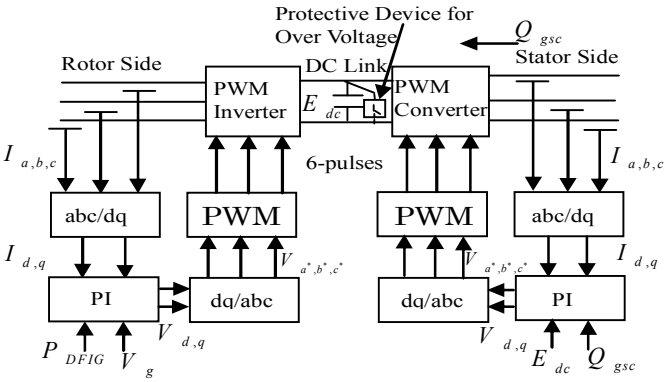

Fig. 7 Circuit configuration of power converters of DFIGs

Table 2. Ratings and Parameters of Excitation Circuit

DC link voltage	1.5kV
DC link capacitor	50,000 μ F
Device for power converter	IGBT
PWM carrier frequency	2kHz
Upper limit of DC voltage (E_{DC_Max})	1.65kV (110%)
Lower limit of DC voltage (E_{DC_Min})	0.75kV (50%)
Short circuit parameter of protective device for over voltage	0.2 ohm

3.1 Rotor Side Converter (RSC) Control

In normal operation (when the grid voltage $V_g > 0.9$), the RSC regulates the developed electric power (P_{DFIG}) and delivers/absorbs reactive power as well by the DFIG. In Fig. 8, θ_{PLL} is the angle of the phase lock loop (PLL), and θ_r is the effective angle for the abc-dq0 and the dq0-qbc transformations. The rotor side converter controls the terminal (grid) voltage to 1.0pu. The d-axis current controls the active power, while the q-axis current controls the reactive power. After a dq0-to-abc transformation, V_{dr}^* and V_{qr}^* are sent to the PWM signal generator. Thus, ${}^*Vr_{abc}$ is the three-phase voltage reference for the rotor side converter output as shown in the configuration circuit of the

converters in Figs. 7 and 8.

3.2 Grid Side Converter (GSC) Control

Figure 8 also shows the control block for the GSC control, where PLL provides the angle θ_{PLL} and θ_s is the effective angle for the abc-to-dq0 (and dq0-to-abc) transformation. The GSC system of the DFIG is used to regulate the DC-link voltage (E_{dc}) to 1.0pu. The d-axis current controls the DC-link voltage, while the q-axis current controls the reactive power of the grid side converter. After a dq0-to-abc transformation, V_q^* and V_d^* are sent to the PWM signal generator. Finally ${}^*Vg_{abc}$ is obtained as a three phase voltage reference at the GSC output.

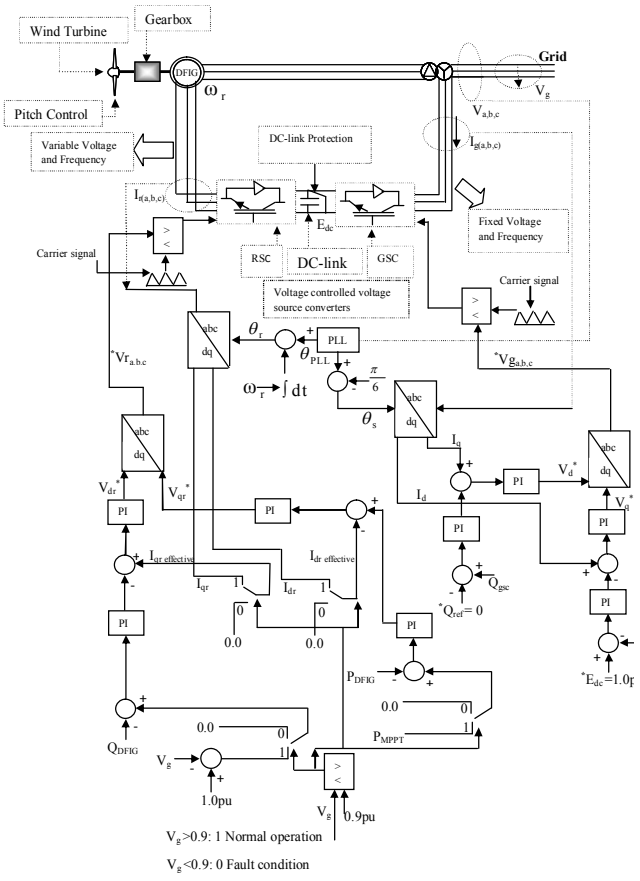

Fig. 8. Control block for rotor and grid side converters

4. Simulation Results

Simulation analyses for a three phase fault at points F1, F2 and F3 shown in Fig. 6 are performed for two cases in PSCAD/EMTDC [21], in which DFIG is installed or is replaced by IG at each wind farm. The fault occurs at 0.1 sec where all wind generators are assumed to be operated under their rated wind speed. The circuit breakers (CB) on the faulted lines are opened at 0.2sec, and finally, at 1.0sec, the circuit breakers are re-closed. Real wind speed data, obtained in Hokkaido Island, Japan, shown in Figs. 9 and 10, respectively, are used in wind farms 1 and 2. Responses of the network variables and some of the wind generators are shown in Figs.11-42.

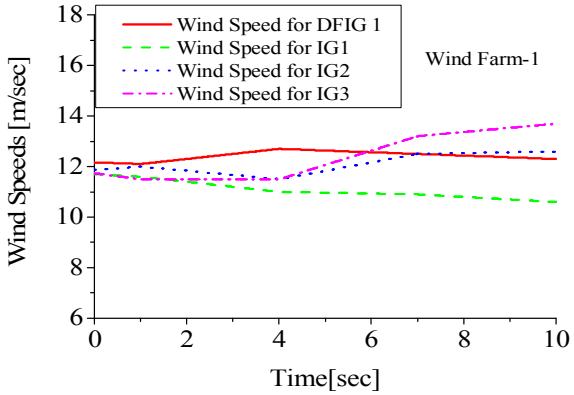

Fig. 9. Wind speeds in wind farm-1.

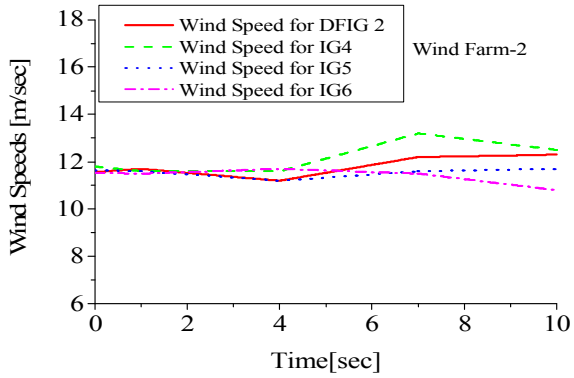

Fig. 10. Wind speeds in wind farm-2.

4.1 Analysis for the fault at point F1

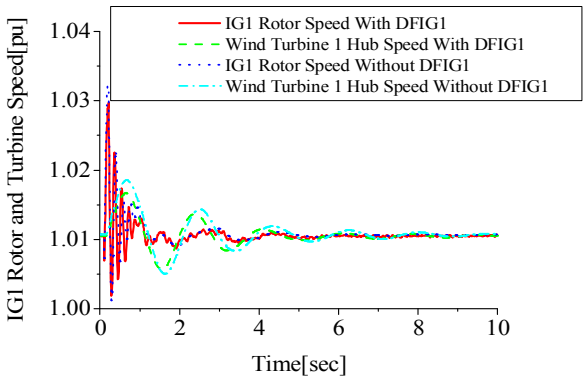

Fig. 11. IG-1 rotor and turbine hub speeds

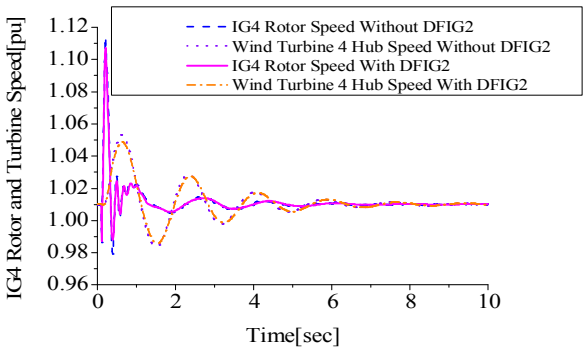

Fig. 12. IG-4 rotor and turbine hub speeds

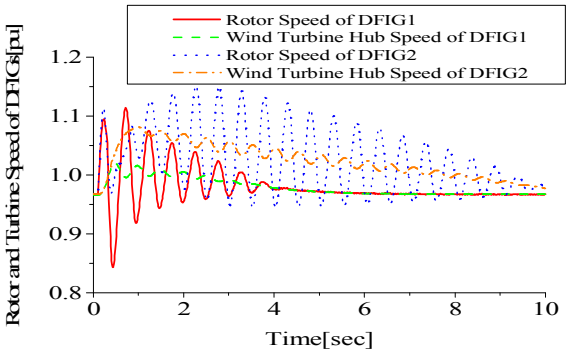

Fig. 13. DFIG-1 and DFIG-2 rotor and turbine hub speeds

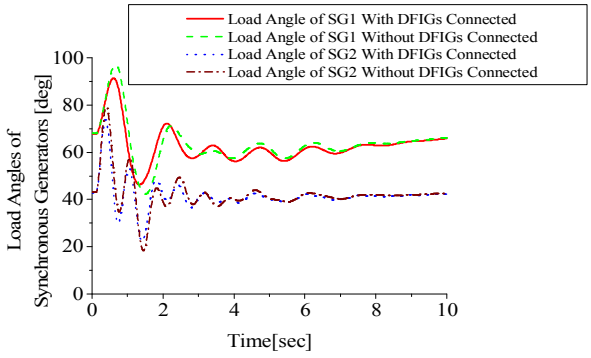

Fig. 14. Load angles of SG-1 and SG-2

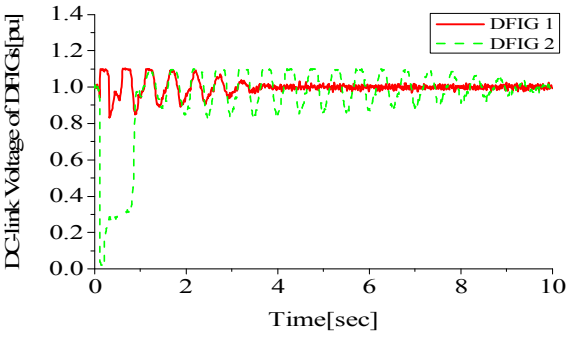

Fig. 15. DC link of voltage of DFIG-1 and DFIG-2

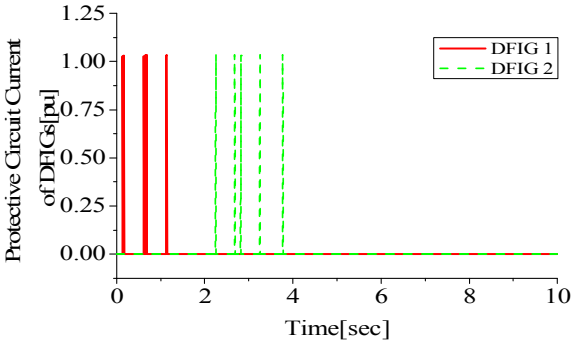

Fig. 16. Current in protective circuit of DFIG-1 and DFIG-2

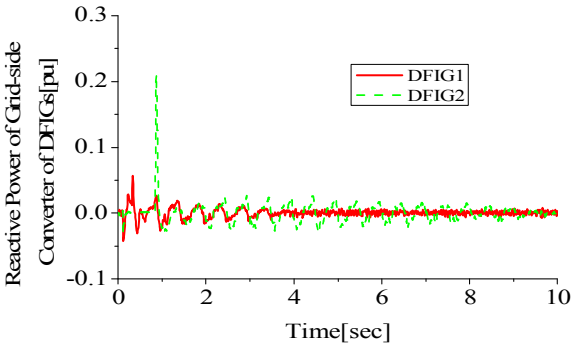

Fig. 17. DFIG-1 and DFIG-2 reactive power of GSC

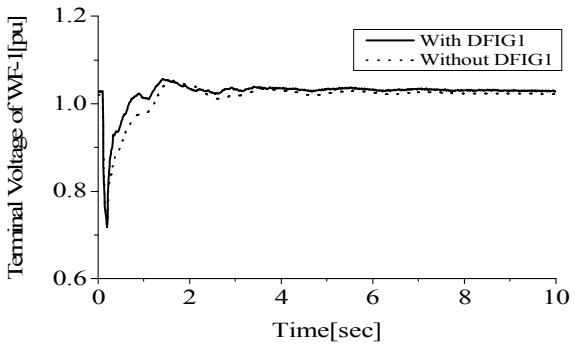

Fig. 18. Terminal voltage (Bus 11) of wind farm-1

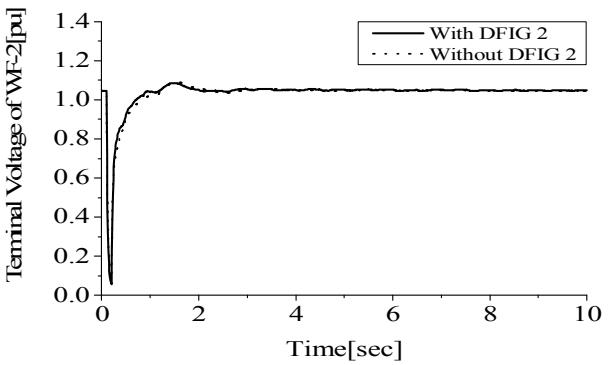

Fig. 19. Terminal voltage (Bus 17) of wind farm-2

4.2 Analysis for the fault point F2

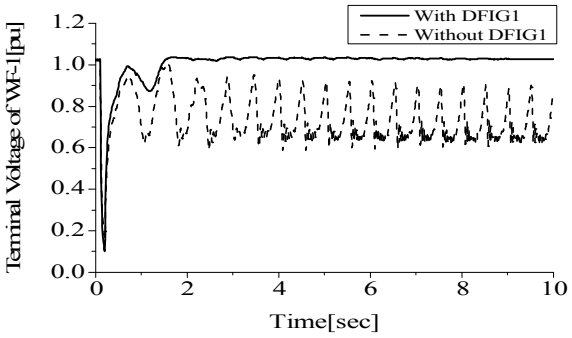

Fig. 20. Terminal voltage (Bus 11) of wind farm-1

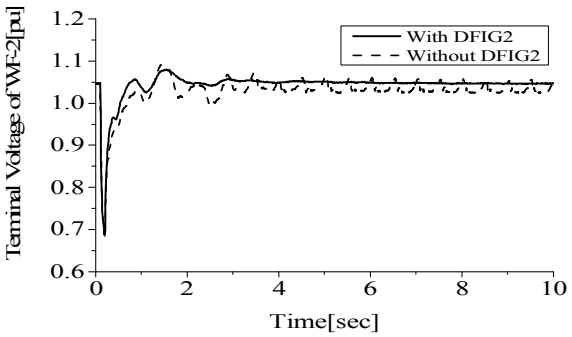

Fig. 21. Terminal voltage (Bus 17) of wind farm-2

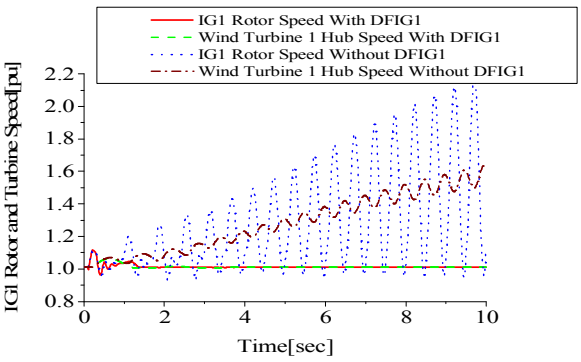

Fig. 22. IG-1 rotor and turbine hub speeds

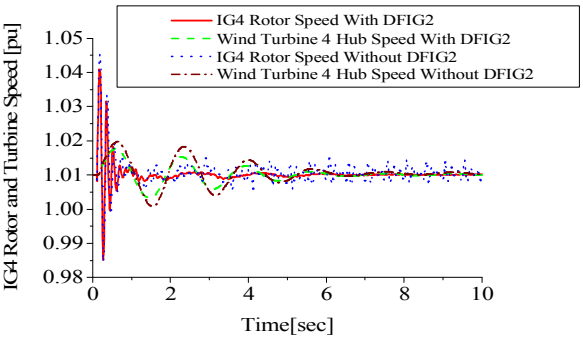

Fig. 23. IG-4 rotor and turbine hub speeds

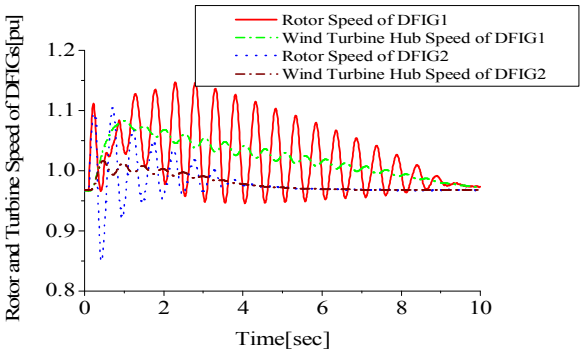

Fig. 24. DFIG-1 and DFIG-2 rotor and turbine hub speeds

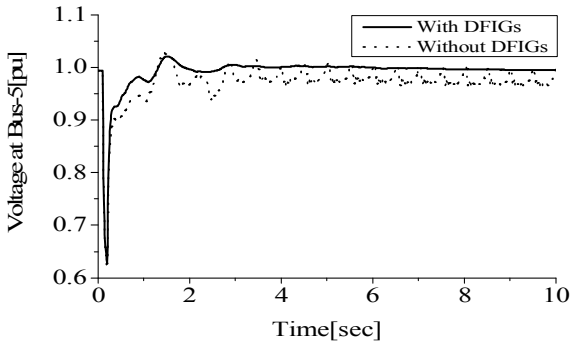

Fig. 25. Voltage at Bus 5

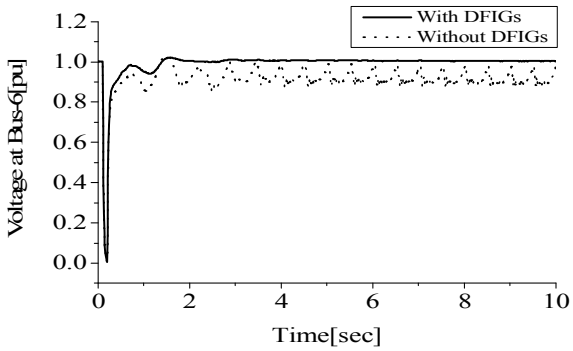

Fig. 26. Voltage at Bus 6

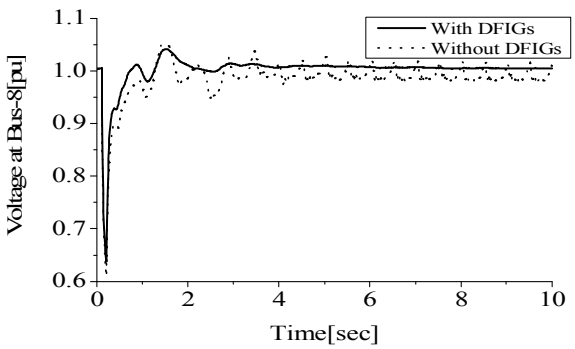

Fig. 27. Voltage at Bus 8

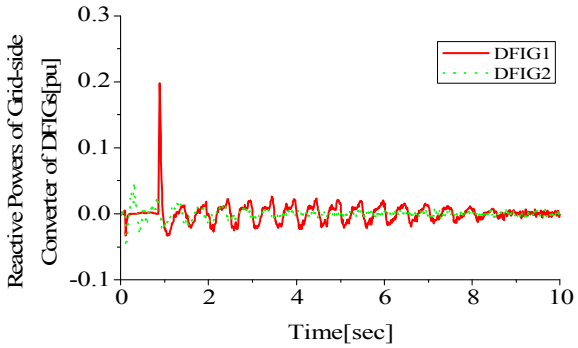

Fig. 28. DFIG-1 and DFIG-2 reactive power of GSC

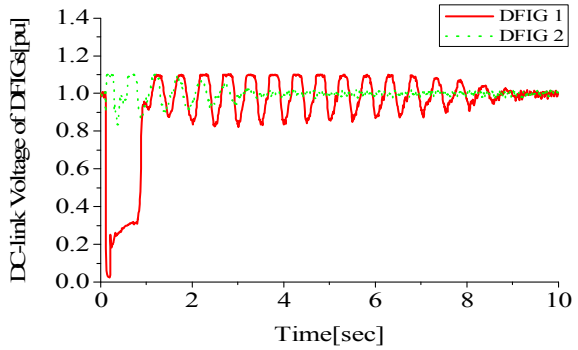

Fig. 29. DC link voltage of DFIG-1 and DFIG-2

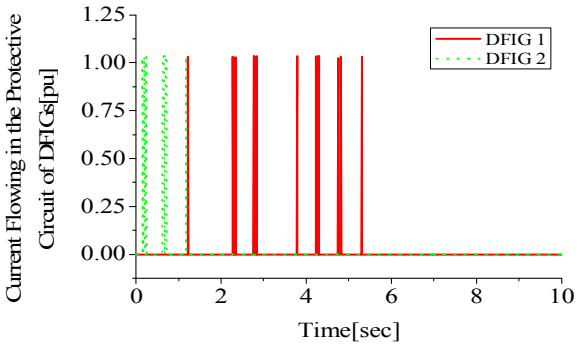

Fig. 30. Current in protective circuit of DFIG-1 and DFIG-2

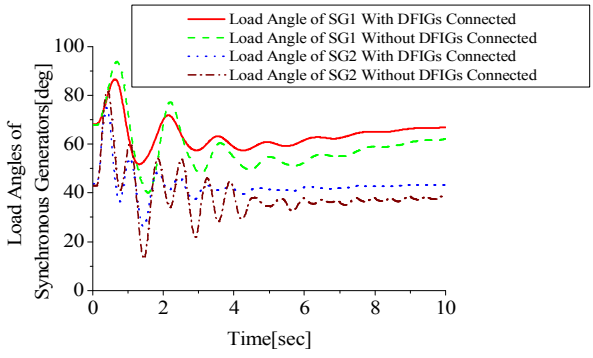

Fig. 31. Load angles of SG-1 and SG-2

4.3 Analysis for the fault point F3

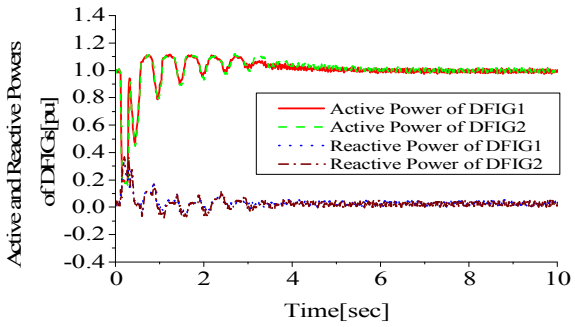

Fig. 32. Active and reactive power of DFIGs

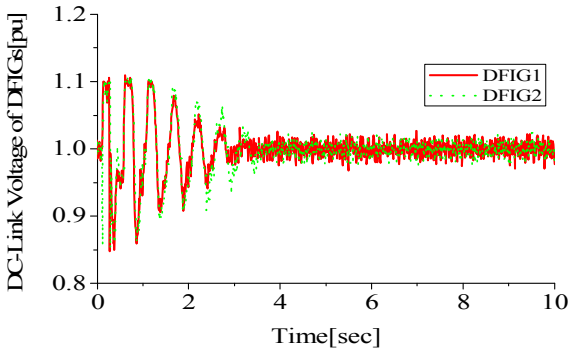

Fig. 33. DC link voltage of DFIG-1 and DFIG-2

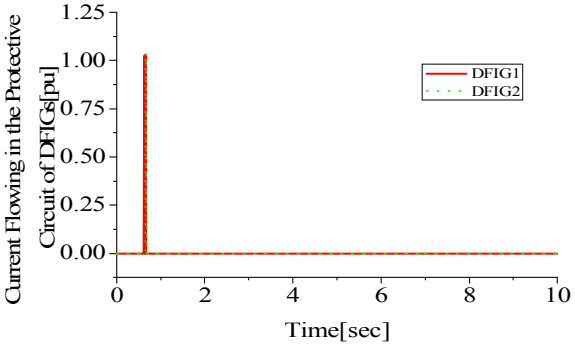

Fig. 34. Current Flowing in protective circuit of DFIGs

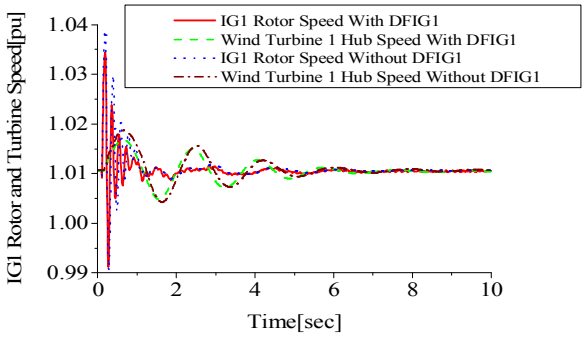

Fig. 35. IG-1 rotor and turbine hub speeds

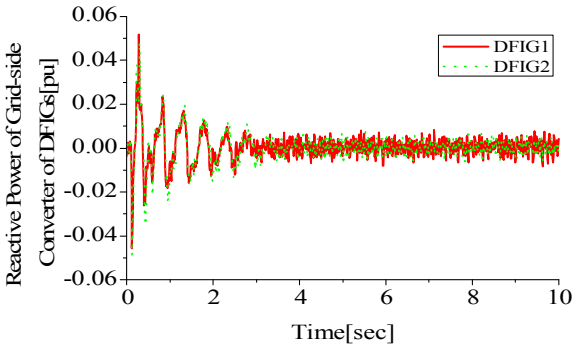

Fig. 36. Reactive power of grid side converter of DFIGs

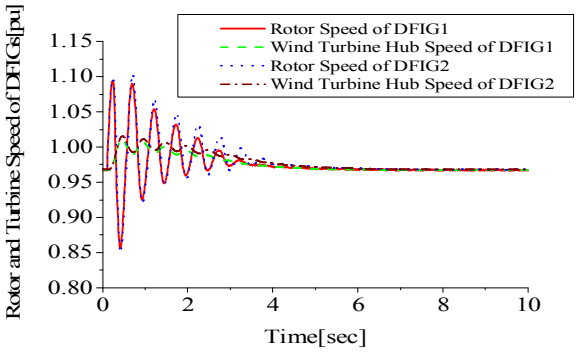

Fig. 37. Rotor and turbine hub speeds of DFIGs

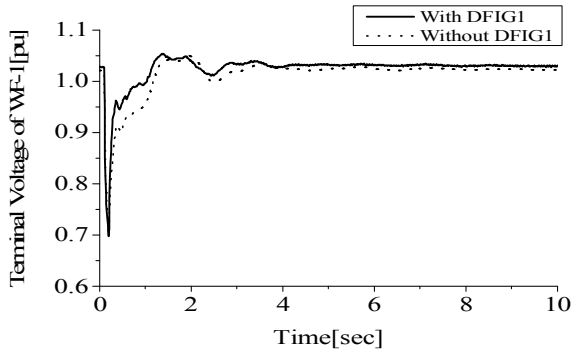

Fig. 38. Terminal voltage of wind farm-1

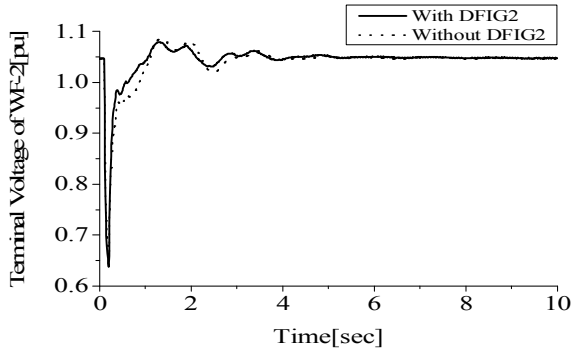

Fig. 39. Terminal voltage of wind farm-2

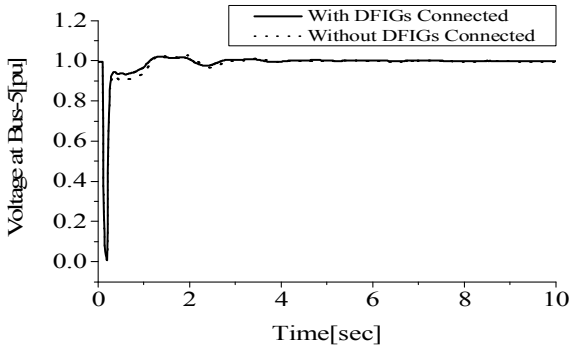

Fig. 40. Terminal voltage at bus 5

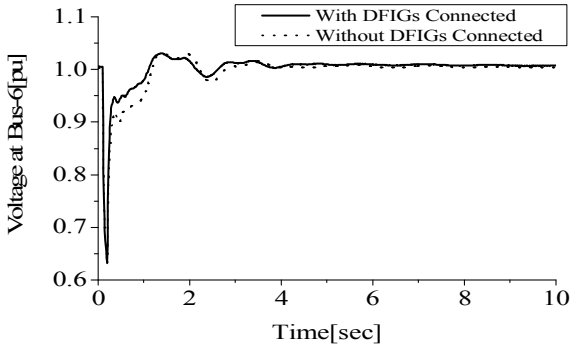

Fig. 41. Terminal voltage at bus 6

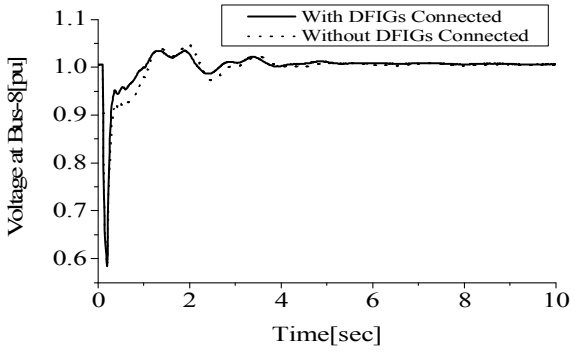

Fig. 42. Terminal voltage at bus 8

Figures 11 and 12 respectively show the responses of IG-1 and IG-4 rotor and turbine speeds for the fault at point F1. The responses for the DFIGs rotor and turbine hub speeds are shown in Fig. 13. Fig. 14 shows the response of the load angles of SG-1 and SG-2. When the DFIGs are connected, better responses of the load angles are achieved. Figs. 15-17 show the DC-link voltage, protection circuit current and the reactive power of the GSC of DFIG-1 and DFIG-2 respectively. The protective current flows only when E_{DC} exceeds $E_{DC\text{-}Max}$. Figs. 18 and 19 show the terminal voltages at wind farm 1 and 2 respectively, where it is evident that the DFIG control was able to recover the

terminal voltages after the grid fault quickly.

The terminal voltage responses of wind farm 1 and 2 for the fault point F2 in Fig. 6 with and without considering DFIG control are shown in Figs. 20 and 21, respectively. When the DFIG control is not considered, the voltage drop occurs at the wind farm and also wind generator terminals. Then, the electromagnetic torques of the IGs drop also as the electromagnetic torque is proportional to the square of the terminal voltage. The mechanical torques of the wind turbines do not change rapidly during the short time interval. As a result, the turbine hub and generator rotors accelerate due to the large difference between the mechanical and electromagnetic torques, and then, the wind generators become unstable as shown in Fig. 22. But if the DFIG control is applied, the necessary reactive power is supplied, and then, the terminal voltages of the wind farm and the electromagnetic torques of the IGs can be restored quickly making the wind generators stable. Fig. 24 shows the response of the DFIG rotor and wind turbine hub speeds, while Figs. 25-27 show the responses of the voltages at bus 5, 6 and 8. Figs. 28-30 show the reactive power of the GSC, DC-link voltage, and protective circuit current of the DFIGs respectively. The load angles of the synchronous generators are shown in Fig. 31, where a better performance was achieved when the DFIGs are present in the wind farms.

Figures 32-34 show the active and reactive powers, DC-link voltage and the current flowing in the protective circuit of the DFIGs for fault point F3. IG-1 rotor and turbine hub speeds, reactive power of the grid side converter and the rotor and turbine hub speeds of the DFIGs, are shown in Figs. 35-37, while Figs. 38 and 39 respectively shows the terminal voltage at wind farm 1 and 2. Figs. 40-42, show the terminal voltages at bus 5, 6 and 8 respectively, where better performance and quick recovery of the terminal voltage responses was achieved when the DFIG control is applied.

5. Conclusion

The DFIG control has been proposed to stabilize a wind farm which is composed of both fixed and variable speed wind turbine generator systems. The effectiveness of the proposed DFIG control is verified by simulation analyses for a severe three-line to ground fault at different fault locations in the multi-machine power system. It has been shown that, if the DFIG control is not available, wind farm composed of induction generators becomes unstable, however, when the DFIG is incorporated in the wind farm adopted with the proposed control, IGs as well as DFIGs in the wind farms become stable. Therefore, it can be concluded that the proposed control method for variable speed wind turbine driving DFIG can effectively enhance the transient stability of wind farms.

Acknowledgements

This work was supported by Japan Gas Corporation Scholarship Foundation (JGC-S)/NIKKI SANEYOSHI and The Petroleum Institute, Abu Dhabi, U.A.E.

References

[1] M. P. Papadopoulos, S. A. Papathanassiou, N. G. Boulaxis, and S. T. Tentzerakis, "Voltage Quality Change by Grid-Connected Wind Turbines," *European Wind Energy Conference*, Nice, France, pp. 783-785, 1999.

[2] B. Pokharel, and W. Gao, "Mitigation of Disturbances in DFIG-based Wind Farm Connected to Weak Distribution System Using STATCOM," *North American Power Symposium (NAPS)*, PP. 1-7, 2010.

[3] J.A., Suul, M. Molinas, and T. Undeland, "STATCOM–based Indirect Torque Control of Induction Machines during Voltage Recovery after Grid Faults," *IEEE Trans. on Power Electronics*, vol. 25, no. 5, pp.1240-1250, 2010.

[4] J. Yu, X. Duan, Y. Tang, and P. Yuan, "Control Scheme Studies of Voltage Source Type Superconducting Magnetic Energy Storage (SMES) Under Asymmetrical Voltage," *IEEE Trans. on Applied Superconductivity*, vol. 12, no.1, pp. 750-753, 2002.

[5] S. M. Muyeen, R. Takahashi, M. H. Ali, T. Murata, and J. Tamura "Transient Stability Augmentation of Power Systems including Wind Farms Using ECS," *IEEE Trans. on Power Systems,* vol. 23, no 3, pp. 1179-1187, 2008.

[6] S. Santos, and H. T. Le, "Fundamental Time-Domain Wind Turbine Models for Wind Power Studies," *Renewable Energy*, vol. 32, pp. 2436-2452, 2007.

[7] R. Takahashi, J. Tamura, M. Futami, M. Kimura and K. Idle, "A New Control Method for Wind Energy Conversion System Using Double Fed Synchronous Generators," *IEEJ Trans. Power and Energy*, Vol.126, no.2, pp.225-235, 2006 (in Japanese).

[8] T. Sun, Z. Chen and F. Blaabjerg, "Transient Stability of DFIG Wind Turbines at an External Short Circuit Fault," *Wind Energy Journal*, vol. 8, pp. 345-360, 2005.

[9] R. D. Fernandez, P.E. Battaiotto, and R. J. Mantz, "Wind Farm Non-Linear Control for Damping Electromechanical Oscillations of Power Systems," *Renewable Energy*, vol. 33, pp. 2258-2265, 2008.

[10] O. Wasynczuk, D. T. Man, and J. P. Sullivan, "Dynamic Behavior of a Class of Wind Turbine Generator during Random Wind Fluctuations," *IEEE Trans. on Power Apparatus and Systems*, vol. PAS-100, no.6, pp. 2837-2845, 1981.

[11] M. Garcia-Garcia, M. P. Comech, J. Sallan, and A. Liombart, "Modeling Wind Farms for Grid Disturbance Studies," *Renewable Energy*, vol. 33, pp. 2109-2121, 2008.

[12] S. Vicatos and J. A. Tegopoulous, "Transient State Analysis of a Doubly Fed Induction Generator Under Three Phase Short Circuit," *IEEE Trans. Energy Convers.*, vol. 6, no. 1, pp. 62-68, March 1991.

[13] S.M. Muyeen, Md. H. Ali, R. Takahashi, T. Murata, J. Tamura, Y. Tomaki, A. Sakahara, and E. Sasano, "Comparative Study on Transient Stability Analysis of Wind Turbine Generator System Using Different Drive Train," *IET Renewable Power Generation*, vol. 1, no.2, pp.131-141, 2007.
[14] Working Group on Prime Mover and Energy Supply Models for System Dynamic Performance Studies, "Dynamic Models for Fossil Fuelled Steam Units on Power System Studies," *IEEE Trans. Power Syst*., vol.6, no.2, pp.753-761, May 1991.
[15] Working Group on Prime Mover and Energy Supply Models for System Dynamic Performance Studies, "Hydraulic Turbine and Turbine control Models for System Dynamic Studies," *IEEE Trans. Power Syst*., vol. 7, no. 1, pp.167-179, Feb. 1992.
[16] *IEEE Recommended Practice for Excitation System Models for Power System Stability Studies*, IEEE Std. 421.5-1992.
[17] A. D. Hasan, and G. Michalke, "Fault Ride-Through Capability of DFIG Wind Turbines," *Renewable Energy*, vol. 32, pp.1594-1610, 2007.
[18] R. G. de Almeida, J. A. Lopez, J. A. L. Barreiros, "Improving Power System Dynamics Behavior Through Doubly Fed Induction Machines Controlled by Static Converter Using Fuzzy Control," *IEEE Trans. Power System*, vol. 19, no. 4, pp. 1942-1950, November, 2004.
[19] J. Morren and S. W. H. de Haan, "Short-circuit Current of Wind Turbines with Doubly Fed Induction Generator," *IEEE Trans. Energy Convers*., vol. 22, no. 1, pp. 174-180, March, 2007.
[20] J. Lopez, E. Gubia, P. Sanchis, X. Roboam, and L. Marroyo, "Wind Turbines Based on Doubly Fed Induction Generator Under Asymmetrical Voltage Dips," *IEEE Trans. Energy Convers*., vol. 23, no. 1, pp. 321-330, March, 2008.
[21] "*PSCAD/EMTDC Manual*", Manitoba HVDC research center, 1994.

Kenneth E. Okedu is currently a Ph.D. student in the department of Electrical and Electronic Engineering, Kitami Institute of Technology, Hokkaido, Japan. He received his B.Sc. and M. Eng. degrees in Electrical and Electronic Engineering from the University of Port Harcourt, Nigeria in 2003 and 2006 respectively. His research interests include the stabilization of wind farm with doubly fed induction wind generator variable speed wind turbine, and power system stability analysis.

S. M. Muyeen received his B.Sc. Eng. degree from Rajshahi University of Engineering and Technology (RUET), Bangladesh, formerly known as Rajshahi Institute of Technology, in 2000, and M. Sc. Eng. and Dr. Eng. degrees from Kitami Institute of Technology, Japan, in 2005 and 2008 respectively, all in Electrical and Electronic Engineering. After completing his Ph.D. program he worked as a Postdoctoral Research Fellow under the versatile banner of Japan Society for the Promotion of Science (JSPS) from 2008-2010 at the Kitami Institute of Technology, Japan. Presently he is working as Assistant Professor in Electrical Engineering department at the Petroleum Institute, UAE. His research interests are power system stability and control, electrical machine, FACTS, energy storage system (ESS), renewable energy, and HVDC system.

Rion Takahashi received the B.Sc. Eng. and Dr. Eng. degrees from Kitami Institute of Technology, Japan, in 1998 and 2006 respectively, all in Electrical and Electronic Engineering. Now he is working as Associate Professor in Department of Electrical and Electronic Engineering, Kitami Institute of Technology. His major research interests include analysis of power system transient, FACTS and wind energy conversion system.

Junji Tamura received his B. Sc. Eng. degree from Muroran Institute of Technology, Japan, in 1979 and M.Sc. Eng. and Dr. Eng. degrees from Hokkaido University, Japan, in 1981 and 1984 respectively, all in Electrical Engineering. He became a lecturer in 1984, an Associate Professor in 1986, and a Professor in 1996 at the Kitami Institute of Technology, Japan. Currently he is a Vice President of the Kitami Institute of Technology.